



# Optical Properties of Gold Nanoparticles on Heavily-Doped Si Substrate Synthesized with an Electrochemical Process

S. Zhu,<sup>a</sup> T. P. Chen,<sup>a,z</sup> Z. Liu,<sup>a</sup> Y. C. Liu,<sup>b</sup> Y. Liu,<sup>c</sup> and S. F. Yu<sup>d</sup>

<sup>a</sup>School of Electrical and Electronics Engineering, Nanyang Technological University, Singapore 639798

<sup>b</sup>Singapore Institute of Manufacturing Technology, Singapore 638075

<sup>c</sup>State Key Laboratory of Electronic Thin Films and Integrated Devices, University of Electronic Science and Technology of China, Chengdu 610054, People's Republic of China

<sup>d</sup>Department of Applied Physics, The Hong Kong Polytechnic University, Hong Kong

Gold nanoparticles on a heavily-doped Si substrate were synthesized through direct electroreduction of bulk  $\text{AuCl}_4^-$  ions. The optical properties of the nanoparticles were determined from ellipsometric analysis. The Lorentz-Drude model was used to represent the effective dielectric function of the gold nanoparticles. A prominent peak at  $\sim 1.7$  eV is identified in the imaginary part  $\epsilon_2$ , which is attributed to the surface plasmon resonance. There are also two minor peaks located at  $\sim 3.1$  and  $\sim 4.2$  eV, respectively, which are related to the interband transitions. The interband transitions are greatly suppressed, which could be due to the modified lattice structures of the nanoparticles.

© 2011 The Electrochemical Society. [DOI: 10.1149/1.3583646] All rights reserved.

Manuscript submitted February 24, 2011; revised manuscript received March 30, 2011. Published April 22, 2011.

Recently, metallic nanoparticles have attracted great interest in the exploitation of the surface plasmon resonance (SPR).<sup>1–3</sup> The excitation of SPR is not only dependent on the extrinsic effects such as size and shape of the nanoparticles, the surrounding dielectric medium, and the interaction between neighboring nanoparticles, it is also related to the dielectric function of the metal nanoparticle itself.<sup>1–4</sup> Among variety of techniques employed for the deposition of metallic nanoparticles, solution-based methods have been used for decades to synthesize metallic nanoparticles (gold, silver).<sup>5,6</sup> This can be done by using a reducing agent together with a metal precursor to form free-standing metallic nanoparticles.<sup>7</sup> Subsequently, the prepared nanoparticles are transferred from the solution to the desired substrate. As a result, a high throughput of metallic nanoparticles with a narrow distribution of diameter can be obtained. However, there are two critical issues restrict the further development of solution-based methods: (1) poor adhesion to the substrate and (2) difficult control of particle coverage and aggregation.<sup>8</sup> Besides the solution-based method, electrodeposition is an alternative technique to synthesize metallic nanoparticles.<sup>8–10</sup> This is an effective technique to deposit metallic nanoparticles on conductive substrate.<sup>8</sup> The particle coverage can be controlled by the applied voltage, while the mean particle diameter can be adjusted by deposition time, concentration and temperature of the solution.<sup>11,12</sup> Owing to its low resistivity, a heavily-doped Si substrate can be used as an electrode in the electrodeposition. The obtained nanoparticles are directly adhered to the Si substrate with good control of coverage and aggregation. Metallic nanoparticles on Si substrate may have applications ranging from sensing<sup>13</sup> to optoelectronics/photronics<sup>14</sup> and surface enhanced spectroscopy.<sup>15</sup> For example, in the application of surface-enhanced Raman spectroscopy (SERS), the silicon substrate exhibits a strong and easily recognized photon band at  $\sim 520$   $\text{cm}^{-1}$ , offering a useful internal reference or standard. In the case of electrodeposition of gold nanoparticles on Si substrate, the gold nanoparticles are firmly adhered to the silicon surface, thus the nanoparticle arrays have very good long-term stability. In addition, unlike glass, there is no interfering fluorescence background from the silicon substrate.

In this study, gold nanoparticles on a heavily-doped Si substrate were synthesized using electrochemical method. The effective dielectric function of the nanoparticles, which is represented by three Lorentz oscillators and a Drude term, was determined from the spectroscopic ellipsometric (SE) analysis. The result shows that the SPR band is red-shifted due to a large average diameter of the nanoparticles, while the amplitudes of the two bands of interband

transition are greatly reduced owing to the changes in the lattice structure.

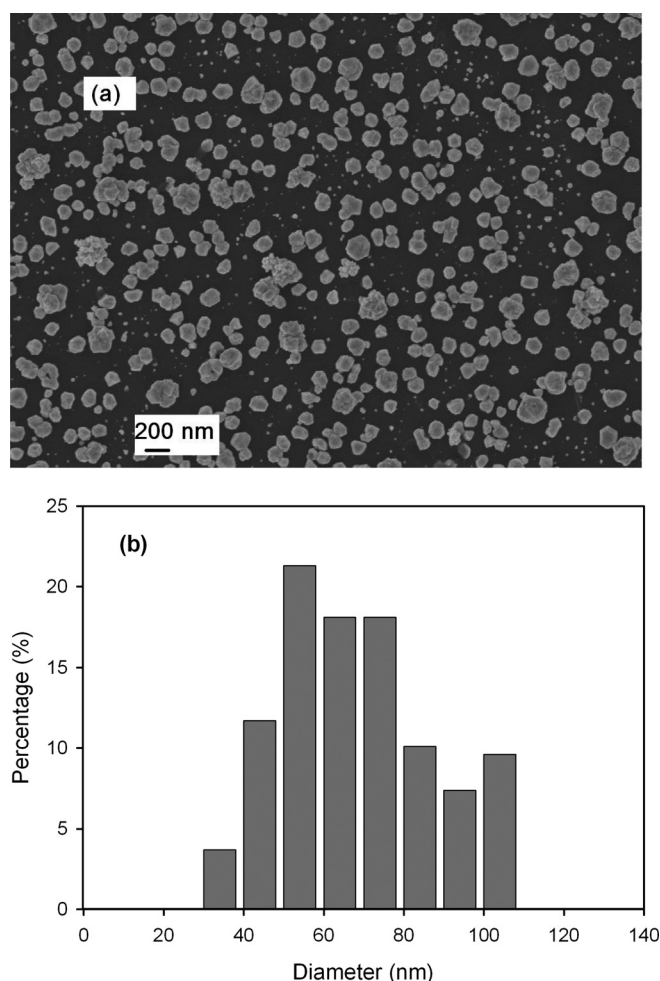
The electrochemical synthesis of gold nanoparticles was carried out by using a two-electrode cell.<sup>8</sup> A  $2 \times 2$   $\text{cm}^2$  platinum mesh was used as the anode. A piece of heavily-doped *p*-type silicon wafer (size:  $\sim 2 \times 2$   $\text{cm}^2$ ; resistivity: 0.001–0.006  $\Omega$  cm), whose native oxide was removed by diluted HF solution, was used as the cathode. The distance between the two electrodes was fixed at 5 cm. All chemicals used in this experiment were of analytic grade and were used without further purification. The electrolytic solutions used in the synthesis of the gold nanoparticles consisted of 0.1  $\text{mol dm}^{-3}$   $\text{KNO}_3$  and  $5.0 \times 10^{-4}$   $\text{mol dm}^{-3}$   $\text{HAuCl}_4$ . A constant current was applied (via a Keithley 2400 source meter) to the electrolysis at room temperature. Scanning electron microscope (SEM) was used to characterize the structural properties of the gold nanoparticles formed on the silicon substrate. Energy-dispersive X-ray spectroscopy (EDX) analysis data of the gold nanoparticle film was recorded by an Oxford Link Isis installed at the SEM (JEOL, JSM-5600LV) system. The SE measurements were performed using a variable angle spectroscopic ellipsometer (J. A. Woollam, Inc). The ellipsometric angles ( $\Psi$  and  $\Delta$ ) were measured in the wavelength range of 300–1100 nm with a step of 5 nm at three different incident angles (i.e., 65, 70, and 75°).

Figure 1(a) shows the representative plane-view SEM image of the gold nanoparticles. It is observed that there are many large particles (tens of nanometers in size) randomly distributed on the substrate surface. In addition, there are also many tiny nanoparticles between the large particles. It is believed that the large particles were formed as a result of the aggregation of the tiny nanoparticles. The surface morphology, size and size distribution of these gold nanoparticles on the Si substrate are strongly dependent on the distance between the anode and cathode electrodes, as well as the duration of deposition. For example, the nanoparticles could be more monodisperse for a short duration of deposition.<sup>8</sup> The particle size distribution is shown in Fig. 1(b). A Gaussian profile was used to fit to the size distribution of the nanoparticles. It is found that the mean particle size and standard deviation are of 61.3 and 21.0 nm respectively. The EDX analysis shown in Fig. 2 confirms that the nanoparticles are indeed gold nanoparticles.

The effective dielectric function of gold nanoparticles can be represented by the Drude term and Lorentz oscillators, which are attributed to the free and bound electron transitions, respectively. The corresponding energy-dependent dielectric function is described as<sup>16,17</sup>

$$\epsilon(E) = \epsilon_{\infty} + \sum_{i=1}^n \frac{A_i}{E_i^2 - E^2 - i\Gamma_i E} - \frac{E_p^2}{E^2 + i\hbar \frac{E}{\tau_D}} \quad [1]$$

<sup>z</sup> E-mail: echentp@ntu.edu.sg



**Figure 1.** (a) A plane-view SEM image of the gold nanoparticles electrochemically synthesized on a heavily-doped Si substrate. (b) Size distribution of the gold nanoparticles.

where  $\epsilon_{\infty}$  is a background constant or an offset,  $A_i$  is the amplitude of the  $i$ th oscillator with the unit of  $(eV)^2$ ,  $E_i$  is the resonance energy with the unit of  $eV$ ,  $\Gamma_i$  is the damping factor of the oscillator with the unit of  $eV$ ,  $E_p$  is the unscreened plasma energy with the unit of

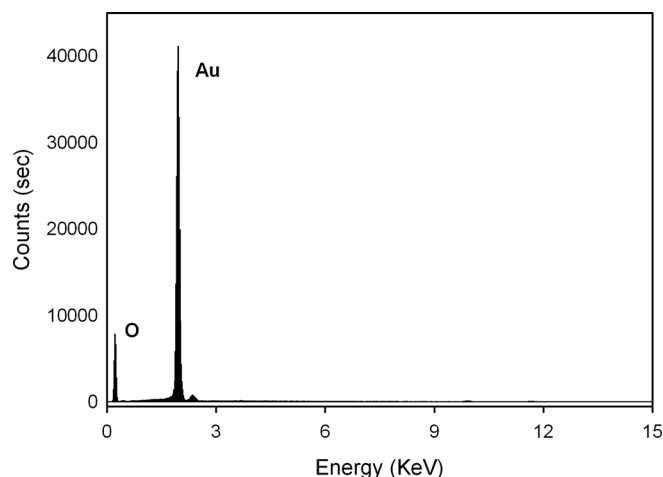


**Figure 2.** EDX analysis of the sample of gold nanoparticles on Si substrate.

$eV$  and  $\tau_D$  is electron relaxation time with unit of  $fs$ . The number of Lorentz oscillators ( $n$ ) is determined to be three (i.e.,  $n=3$ ), as two oscillators model the interband transitions and the other oscillator models the surface plasmon resonance. On the other hand, the gold nanoparticle layer is considered as a composite layer consisting of the gold nanoparticles and voids, whose effective dielectric function can be calculated using the Maxwell-Garnett effective medium approximation (EMA).<sup>16,17</sup> As shown in Fig. 1(a), the surface coverage of the gold nanoparticles is less than 30%, thus, the volume fraction of the voids should be larger than the volume of the gold nanoparticles. In fact, the volume fractions of gold nanoparticles and voids yielded from the SE spectral fitting described below are  $\sim 20$  and  $\sim 80\%$ , respectively. Therefore, the gold nanoparticles should be treated as an inclusion in the EMA.

The spectral fitting to the experimental ellipsometric angles ( $\Psi$  and  $\Delta$ ) was performed by adjusting the parameters in Eq. (1) together with the volume fraction of the gold nanoparticles and the composite layer thickness to minimize the mean-square error between the measured and calculated ellipsometric angles.<sup>18</sup> Figure 3 shows the spectral fittings to the experimental data at different incident angles. All spectral features can be fitted excellently. The Lorentz model parameters obtained from the fittings are listed in Table I.

Figure 4 shows the effective dielectric function  $\epsilon$  of the gold nanoparticles as a function of photon energy. A prominent peak at  $\sim 1.7$  eV can be identified in the imaginary part  $\epsilon_2$ , while two minor peaks at  $\sim 3.1$  and  $\sim 4.2$  eV can be barely observed. All these peak positions are consistent with the resonance energies of the Lorentz oscillators yielded from the spectral fittings (see Table I). The real part  $\epsilon_1$  of the effective dielectric function is positive over the entire

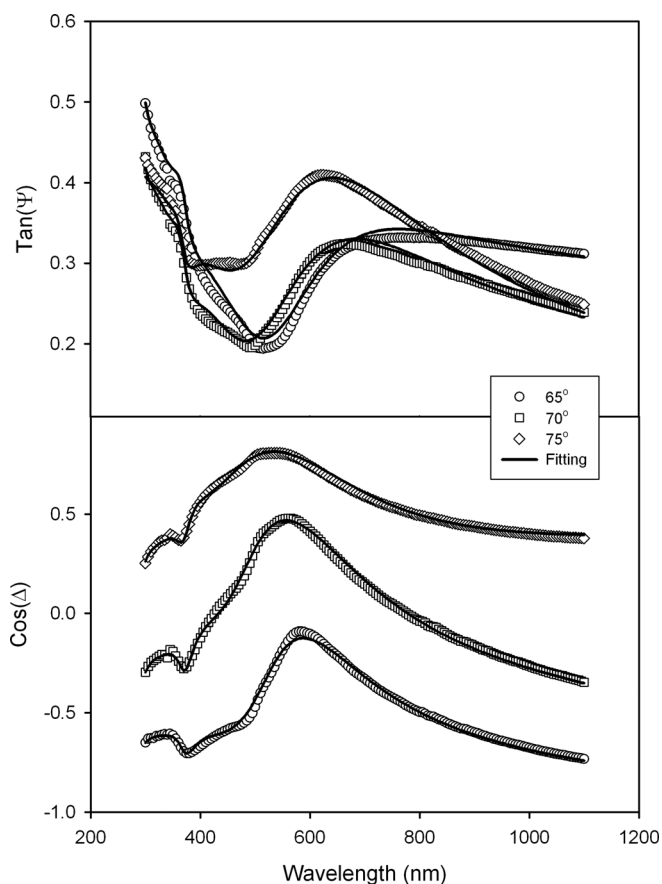


**Figure 3.** Spectral fittings to the experimental ellipsometric data at different incident angles.

**Table I. Values of the Lorentz oscillator parameters of Eq. 1 yielded from the SE fittings.**

	Lorentz 1	Lorentz 2	Lorentz 3
$A_i$ (eV <sup>2</sup> )	4.48	1.29	4.70
$E_i$ (eV)	1.73	3.07	4.32
$\Gamma_i$ (eV)	0.87	1.20	2.70

spectral range of the ellipsometric measurement, which is consistent with the previous study of discrete metal islands.<sup>19,20</sup>

The contributions of the three Lorentz oscillators to the dielectric function are also shown in Fig. 4. The first oscillator with the resonance energy of  $\sim 1.7$  eV is associated with the surface plasmon resonance (SPR) of the gold nanoparticles. As the size of the gold nanoparticle becomes much smaller than the wavelength of incident light, light can easily penetrate through the whole nanoparticle, which will cause a redistribution of free electrons with respect to the positively charge ions. The formed metallic lattices can be considered as resonators, and their oscillation amplitude will be magnified if excited resonantly.<sup>21</sup> In general, the SPR band is determined by the size and shape of the nanoparticles, as well as the surrounding dielectric medium. In our study, the SPR band is located at  $\sim 1.7$  eV. This energy is lower than the commonly proposed characteristic band position ( $\sim 2.2$  eV).<sup>22,23</sup> The red-shifted SPR band observed here can be explained by the large average diameter of the nanoparticles.<sup>23</sup> Image charge effect from Si substrate was also proposed for a red-shifted SPR band.<sup>16</sup> However, the image charge effect might not play an important role here, because the Si substrate could have been oxidized during the electroreduction process as a clear O signal

was observed in the EDX analysis (see Fig. 3). On the other hand, the Lorentz oscillators with the resonance energies of  $\sim 3.1$  and  $\sim 4.2$  eV are attributed to the interband transitions. The oscillator of 3.1 eV corresponds to the transitions from the uppermost 5d-valence electron bands to states in the *s*, *p* bands just above the Fermi level; while the oscillator of 4.2 eV represents the transitions from the lower-lying *d* bands to band 6 and from *s*, *p* states in band 6 to *s*-, *p*-like states in band 7.<sup>24</sup> The transitions would be affected by the structures of the gold nanoparticles. As can be concluded from Fig. 4, the amplitudes of the two bands of interband transitions are very small. This should be related to the structures of the gold nanoparticles, but the detail is not known yet.

The refractive index *n* and the extinction coefficient *k* of the gold nanoparticles can be obtained from the calculation using the dielectric function shown in Fig. 4 with the following equations

$$n = \sqrt{\frac{\sqrt{\varepsilon_1^2 + \varepsilon_2^2} + \varepsilon_1}{2}} \quad [2]$$

$$k = \sqrt{\frac{\sqrt{\varepsilon_1^2 + \varepsilon_2^2} - \varepsilon_1}{2}}$$

where  $\varepsilon_1$  and  $\varepsilon_2$  are the real and imaginary parts of the dielectric function, respectively. The refractive index and extinction coefficient of the gold nanoparticles as a function of photon energy obtained from the above calculation are shown in Fig. 5. As can be observed in the figure, the refractive index and extinction coefficient of the gold nanoparticles are very different from that of a gold film.<sup>25</sup> The difference is due to the large contribution of the surface plasmon resonance of the gold nanoparticles and the significant

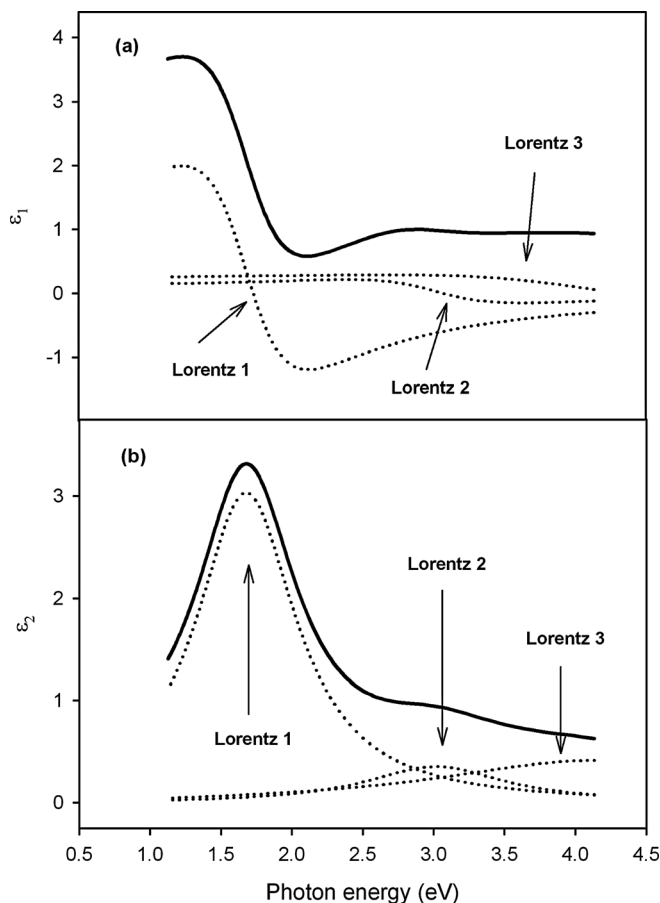


**Figure 4.** Effective dielectric function of the gold nanoparticles: (a) real part  $\varepsilon_1$  and (b) imaginary part  $\varepsilon_2$ . The contributions of the three Lorentz oscillators are shown in the figure also.

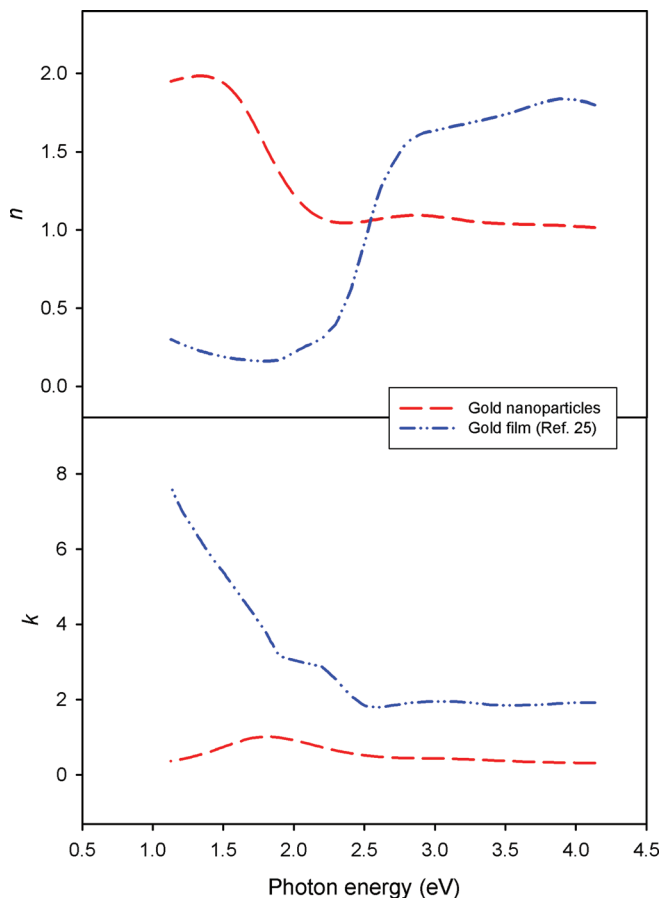


**Figure 5.** (Color online) Refractive index *n* and extinction coefficient *k* of the gold nanoparticles. The optical constants of a gold film (Ref. 25) are also shown in the figure for comparison.

changes in the interband transitions associated with the structures (e.g., size and shape) of the nanoparticles, as discussed above.

In conclusion, gold nanoparticles have been synthesized on a heavily-doped Si substrate using electrochemical approach. The morphology of the nanoparticles can be manipulated by adjusting the distance between the anode and cathode of the electrochemical cell as well as the process time. The effective dielectric function of the gold nanoparticles can be modeled with three Lorentz oscillators together with a Drude term. A prominent peak in the imaginary part  $\epsilon_2$ , which is attributed to the surface plasmon resonance of the gold nanoparticles, is observed. Besides, two minor Lorentz bands due to the interband transitions are also identified.

### Acknowledgments

This work has been financially supported by National Research Foundation of Singapore (NRF-G-CRP 2007-01). Y. Liu acknowledges NSFC under project No. 60806040, and the Grant under project No. 2008ZC80.

### References

1. N. J. Halas, *Nano Lett.*, **10**, 3816 (2010).
2. E. Hutter and J. H. Fendler, *Adv. Mater.*, **16**, 1685 (2004).
3. W. A. Murray and W. L. Barnes, *Adv. Mater.*, **19**, 3771 (2007).
4. S. Link and M. A. El-Sayed, *Annu. Rev. Phys. Chem.*, **54**, 331 (2003).
5. E. S. Kooij, H. Wormeester, E. A. M. Brouwer, E. van Vroonhoven, A. van Silfhout, and B. Poelsema, *Langmuir* **18**, 4401 (2002).
6. D. V. Goia, *J. Mater. Chem.*, **14**, 451 (2004).
7. A. N. Shipway, E. Katz, and I. Willner, *ChemPhysChem*, **1**, 18 (2000).
8. D. A. Brevnov and C. Bungay, *J. Phys. Chem. B*, **109**, 14529 (2005).
9. S. X. Huang, H. Y. Ma, X. K. Zhang, F. F. Yong, X. L. Feng, W. Pan, X. N. Wang, Y. Wang, and S. H. Chen, *J. Phys. Chem. B*, **109**, 19823 (2005).
10. X. Jiang, R. Ferrigno, M. Mrksich, and G. M. Whitesides, *J. Am. Chem. Soc.*, **125**, 2366 (2003).
11. A. Radisic, G. Oskam, and P. C. Searson, *J. Electrochem. Soc.*, **151**, C369 (2004).
12. R. M. Penner, *J. Phys. Chem. B*, **106**, 3339 (2002).
13. J. Spadavecchia, P. Prete, N. Lovergine, L. Tapfer, and R. Rella, *J. Phys. Chem. B*, **109**, 17347 (2005).
14. S. Pillai, K. R. Catchpole, T. Trupke, and M. A. Green, *J. Appl. Phys.*, **101**, 093105 (2007).
15. Z. H. Zhu, T. Zhu, and Z. F. Liu, *Nanotechnology*, **15**, 357 (2004).
16. S. Zhu, T. P. Chen, Z. H. Cen, E. S. M. Goh, S. F. Yu, Y. C. Liu, and Y. Liu, *Opt. Express*, **18**, 21926 (2010).
17. S. Zhu, T. P. Chen, Z. H. Cen, Y. C. Liu, and Y. Liu, *Electrochem. Solid-State Lett.*, **13**, K39 (2010).
18. L. Ding, T. P. Chen, Y. Liu, C. Y. Ng, and S. Fung, *Phys. Rev. B*, **72**, 125419 (2005).
19. A. J. De Vries, E. S. Kooij, H. Wormeester, A. A. Mewe, and B. Poelsema, *J. Appl. Phys.*, **101**, 053703 (2007).
20. T. W. H. Oates, D. R. McKenzie, and M. M. M. Bilek, *Phys. Rev. B*, **70**, 195406 (2004).
21. V. M. Shalaev, *Nanophotonics With Surface Plasmons*, Elsevier, Amsterdam, Boston (2007).
22. E. S. Kooij and B. Poelsema, *Phys. Chem. Chem. Phys.*, **8**, 3349 (2006).
23. S. Zhu, T. P. Chen, Y. C. Liu, S. F. Yu, and Y. Liu, *Electrochem. Solid-State Lett.*, **13**, K96 (2010).
24. M. Losurdo, M. M. Giangregorio, G. V. Bianco, A. A. Suvorova, C. Kong, S. Rubanov, P. Capezzuto, J. Humlicek, and G. Bruno, *Phys. Rev. B*, **82**, 155451 (2010).
25. E. D. Palik, *Handbook of Optical Constants of Solids*, Academic, Orlando, FL (1985).